JOURNAL OF CATALYSIS 46, 167–189 (1977)

The Hydrogenation of CO and CO_2 over Polycrystalline Rhodium: Correlation of Surface Composition, Kinetics and Product Distributions

B. A. SEXTON AND G. A. SOMORJAI

Materials and Molecular Research Division, Lawrence Berkeley Laboratory and Department of Chemistry, University of California, Berkeley, California 94720

Received July 16, 1976; revised October 18, 1976

Rhodium, in the form of a small surface area ($\sim$1 cm^2) polycrystalline foil was used to study the CO–H_2 and CO_2–H_2 reactions at low ($\sim 10^{-4}$ Torr) and at high (700 Torr) pressures in the same apparatus. Reaction rates and product distributions were monitored with a mass spectrometer and a gas chromatograph, respectively, and the surface composition was determined by Auger electron spectroscopy. The various binding states of CO were studied by thermal desorption. Under reaction conditions (250–350°C, 700 Torr) the surface is covered with a catalytically active carbonaceous deposit while some oxygen is located below the surface. No surface oxygen was detectable after reaction as the removal of chemisorbed species by either the CO–O_2 or H_2–O_2 reactions was rapid at low temperatures. Carbon monoxide was found to adsorb in molecular form on clean Rh surfaces, but partly dissociated on surfaces pretreated in CO, or by heating in the presence of gaseous CO. Co-adsorption of H_2/CO mixtures at low pressures increased the amount of molecular CO but no changes in CO binding energy were observed.

At low pressures (10^{-4} Torr) the equilibrium hydrocarbon partial pressures from the CO–H_2 and CO_2–H_2 reactions are too low to be detectable. At high pressures (700 Torr), the reaction rates, activation energy (24 $\pm$ 3 kcal) and product distributions from the small surface area Rh foil are nearly identical to that obtained on a dispersed rhodium catalyst. The CO_2–H_2 reaction produces methane exclusively and with a lower activation energy (16 $\pm$ 2 kcal) than for the CO–H_2 reaction. Pretreatment of the clean surface changes the product distribution and the rates in both reactions. Pretreatment with acetylene deposits surface carbon and reduces methanation, but not chain growth in the CO–H_2 reaction (a higher percentage of C_2 and C_3 products). Pretreating with oxygen dissolves oxygen in the bulk and increases the methanation rate by up to a factor of five over the clean surface. It appears that active rhodium–carbon–oxygen complexes form at the surface and rehydrogenate to yield the various products.

I. INTRODUCTION

The synthesis of organic compounds from carbon monoxide and hydrogen mixtures over transition metal catalysts has been described extensively (*1*) in the literature since the initial publication in 1902 by Sabatier and Senderens. Most of the chemical studies concentrated on maximizing the yields and optimizing the selectivity for the main reactions; methanation (*2*), the methanol synthesis (*3*), and the synthesis of higher molecular weight hydrocarbons [Fischer–Tropsch reaction (*4*)].

The formation of hydrocarbons from CO–H_2 mixtures is thermodynamically favorable, although higher pressures (in excess of 1 atm) are necessary to facilitate the formation of higher molecular weight products. (The pressure dependence of the

ISSN 0021-9517

thermodynamics of hydrocarbon production is described in the Appendix.) Thermodynamic equilibrium between the reactants and the many possible products is not established even at the high pressures commonly employed. Thus, surface reactions determine the rate and product distribution, and it is important that we investigate the elementary steps of the surface reactions on the atomic scale to learn how to control the kinetics and the selectivity.

The purpose of our studies is to correlate the reactivity of the catalyst surface with its atomic structure and chemical composition. We have developed new instrumentation that permits the characterization of the catalyst surface structure and composition in ultrahigh vacuum by electron scattering techniques (low energy electron diffraction (LEED) and Auger electron spectroscopy (AES)). Then, using the same apparatus we can carry out chemisorption studies and reaction studies at low pressures ($\sim 10^{-4}$ Torr) and at high pressures (1–100 atm). This instrument is described in detail below.

This paper reports studies of the reaction of CO and H_2, and CO_2 and H_2 to form hydrocarbons, using polycrystalline rhodium as a catalyst. We shall show that the kinetics of methanation on this metal foil of about ~ 1 cm^2 area, is in excellent agreement with the results obtained on dispersed and supported rhodium catalysts. Thus, small area metal samples can be used as models of Fischer–Tropsch catalysts. We have determined the specific reaction rates (turnover numbers) and product distributions under a variety of experimental conditions. The surface reaction layer was characterized before and after the high pressure runs by AES and thermal desorption measurements.

We have found evidence for the presence of both molecular and dissociated CO on the surface, during the synthesis. The active rhodium surface develops a carbonaceous deposit, while chemisorbed oxygen is rapidly removed from the surface layer by CO and H_2. Both carbon and oxygen also appear to be located below the metal surface. By changing the composition and/or structure of the rhodium–carbon surface complex by pretreatment (with acetylene or oxygen) both the reaction rate and the product distribution can be markedly altered. The CO_2–H_2 reaction yielded methane predominantly, in contrast to the much

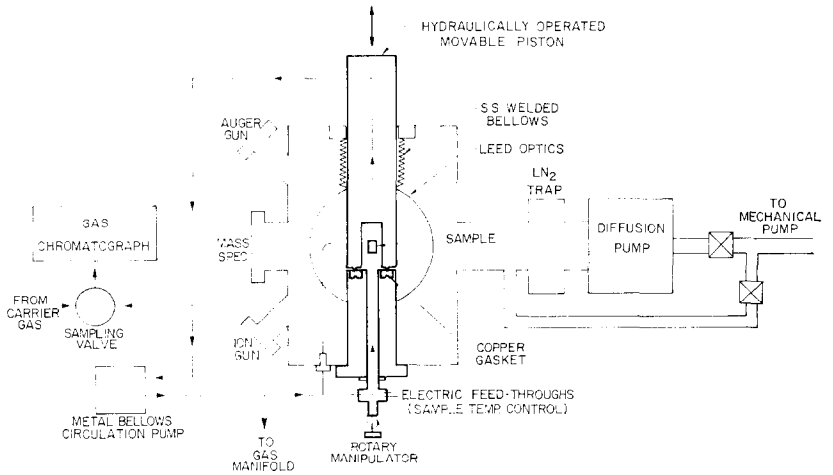

FIG. 1. Schematic of UHV surface analysis system equipped with sample isolation cell for catalytic studies at high pressures (1–100 atm) and low pressures (10^{-8}–10^{-4} Torr).

broader product distribution obtained from CO–H_2 reactions under the same conditions.

II. EXPERIMENTAL METHODS

The apparatus used in this study has been described in detail elsewhere (*5*); and it is shown schematically in Fig. 1. Essentially, it is an UHV surface analysis instrument incorporating an internal isolation cell, for catalytic studies at pressures from 1–100 atm. In this work, this cell was operated at 700 Torr during the high pressure experiments, and for low pressure studies (10^{-8}–10^{-4} Torr), the UHV chamber was used as the reaction vessel.

The rhodium samples were small, rectangular pieces of 0.005 in. thick, high purity foil, with surface areas <1 cm^2, mounted on either a thin tantalum or rhodium holder. For quantitative measurement of reaction rates and thermal desorption on only one side of the foil, tantalum was used as an inert mask to cover unwanted portions. In other experiments, such as measurement of surface composition, a rhodium holder was used. For quantitative measurements of rates, masking of the rhodium foil was necessary, because only one side was accessible to the ion bombardment gun.

The tantalum or rhodium holder was spotwelded to two stainless steel heating rods, which were connected to the copper bars of the manipulator. As shown in Fig. 1, the manipulator provided a 180° axial rotation of the sample, and was enclosed in the 0.5 in. i.d. lower port of the isolation cell. A Chromel–Alumel thermocouple was spotwelded to the rear of the sample. Rotary movement was achieved via a Teflon compression-sealed stainless steel shaft. This seal was leak-free in the UHV environment, as well as having the capability of operation at high pressures (<5000 psi). It was essential to keep the internal volume of the manipulator assembly to an absolute minimum, as it formed part of the reaction cell at high pressures. Commercial manipulators were rejected on the basis of excessive internal volume, and lack of a high pressure capability (>1 atm internal pressure).

As shown in Fig. 1, the Rh sample was located at the focus of the LEED optics in the center of the UHV chamber, and a 180° rotation was possible to direct the surface toward the quadrupole mass spectrometer for thermal desorption measurements, the sputter ion gun for cleaning, and the Auger gun for surface analysis. In the case of single crystals, LEED observations are also possible using this manipulator, although none are reported in this work.

The UHV chamber was pumped by a fast, (1000 liters sec^{-1}) 6 in. diffusion pump, with a 20 hr liquid nitrogen trap, and a titanium sublimation pump. This pumping combination was chosen to handle the large gas loads of CO and H_2 encountered when opening the high pressure cell, and to reduce the pump-down time before analysis of the surface after a high pressure run. After bakeout, the system base pressure was $\leqslant 1 \times 10^{-9}$ Torr, which was adequate for sample cleaning purposes, and low pressure adsorption and catalysis experiments (10^{-9}–10^{-4} Torr).

The high pressure isolation cell, which is shown in Fig. 1 in the closed position, was a stainless steel cylinder with a small ($\sim$30 ml) cavity which enclosed the Rh sample, and was sealed by a copper gasket situated below the sample, on the fixed portion of the cell. This cylinder was attached to a small hydraulic press situated on top of the apparatus, which moved it up and down. The whole assembly had a total travel of about 3 in., and was bellows sealed, to maintain UHV during movement. The sealing elements of the cell were rounded knife edges, which permitted many seals using the same gasket, and approximately 2000 psi hydraulic pressure was needed to provide a totally leak-free seal. The gasket, which was a commercial "Mini-Conflat" copper type, was softened by annealing

before use. This seal has been in service for over 100 experiments without replacement, at 1 atm internal operation, with an external vacuum of $\sim 10^{-9}$ Torr.

Gases were admitted to, and circulated through the isolation cell by means of ports along the axis of the cell. As stated previously, the lower port enclosed the rotary manipulator, and gas could be circulated out through the upper port in the movable piston, and back into the manipulator, via an external metal bellows pump (Metal Bellows Corp. Model MB10). This external loop also incorporated a small volume (0.1 ml) gas chromatography sampling valve, which extracted samples for analysis into the gas chromatograph (Perkin-Elmer Model 3920). The isolation cell and external gas circulation route therefore were operated as a small volume (100 ± 5 ml) stirred batch reactor.

Admission of a H_2/CO gas mixture to the reactor (cell + loop) was accomplished via a sorption-pumped manifold, which had inlets for H_2, CO, CO_2, Ar and calibration gases. This manifold served also to admit gases to the UHV chamber for low pressure experiments. All gases were high purity, from Matheson Gas Products, and no further purification was attempted. Gas mixtures were usually prepared in the manifold, then expanded into the reactor, or bled into the UHV system.

For low pressure catalysis studies (10^{-8}–10^{-4} Torr), the isolation cell was raised to the open position, and the Rh sample was cleaned by Ar^+ ion bombardment (2 keV ions 5×10^{-5} Torr, 20 μA) and annealing at 1000°C in UHV. After AES analysis, gases could be admitted to the chamber via variable leak valves, and adsorption experiments, or catalytic reactions were carried out. For a catalysis experiment, the chamber was operated as a flow system, in which a dynamic pressure was maintained between 10^{-8} and 10^{-4} Torr by reducing the pumping speed with partial closure of the gate valve, while the sample was heated to a desired reaction temperature. Reaction products were detected with the quadrupole mass spectrometer, and reaction rates and product distributions were determined by analysis of the cracking patterns. The maximum pressure (10^{-4} Torr), that could be employed in these experiments is determined by the mass spectrometer detection. One advantage of this method was that *in situ* AES or LEED analyses of the catalyst surface were possible during the reaction, due to the sufficiently long electron mean free path at these reduced pressures.

For a high pressure (1 atm) catalysis experiment, the sample was usually cleaned by Ar^+ ion bombardment (2000 eV, 20 μA) and annealing, and following surface analysis, the isolation cell was lowered and sealed. (At this point, it was possible to demount the entire manipulator assembly and change samples, without breaking UHV in the main chamber.) Gases were pre-mixed in the manifold, then expanded into the cell and evacuated loop, to a total pressure of 700 Torr as measured on an absolute pressure dial gauge. The circulation pump was started and the loop was isolated from the manifold via a valve. Several preliminary gc samples were taken, then the sample temperature was adjusted to reaction conditions (200–450°C) by a proportional temperature controller, which compensated for variations in temperature due to resistance changes and gas flow variations. Regulation was possible to within 1 or 2°C and the Chromel–Alumel thermocouple output was measured on a Keithley millivoltmeter.

Periodically, samples were extracted into the gas chromatograph for analysis. Negligible change in total pressure occurred due to sample extraction ($\sim 0.1\%$). After reaction, the gases were evacuated from the central cell and loop by the sorption pumps, and the cell was then isolated from the loop, and reexposed to UHV by raising the upper cell cylinder. The pressure was usually in the low 10^{-8} range within 10 min and below 1×10^{-8} Torr within 30 min.

Surface analysis, and thermal desorption measurements were carried out, and the sample could then be re-cleaned for a new run. A series of blank experiments was conducted and it was found that there was negligible hydrocarbon production from CO–H_2 mixtures on the tantalum support, thermocouple, or stainless steel walls.

Gas chromatography samples at high pressures (700 Torr) were analyzed over Chromosorb 102 columns, which resolved all of the lower molecular weight hydrocarbons adequately. A consequence of the use of small surface area (<1 cm^2) catalyst samples was that conversions were about 0.1%, and flame ionization detection was necessary to detect the product formation. Product detection and analysis was simplified by the fact that H_2, CO, and CO_2 were not detectable in the hydrogen flame, although regrettably, other products such as H_2O were also not detectable.

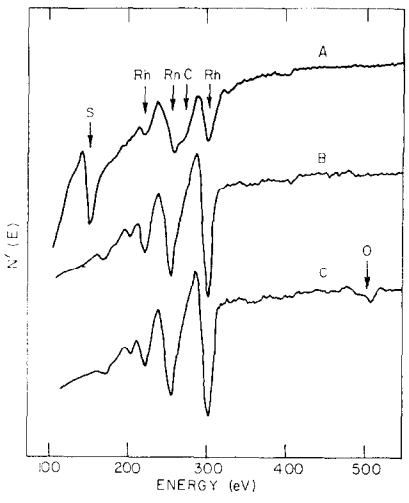

FIG. 2. Auger spectra of rhodium surface: (A) before cleaning; (B) after cleaning with 2000 eV Ar^+ ions and annealing at 1000°C; (C) after treatment with oxygen (1×10^{-7} Torr, 500°C, 10 min).

III. RESULTS

A. Low Pressure Studies

1. Preparation of Clean Rhodium Surfaces

The Auger spectra of the Rh surface before and after cleaning are shown in Fig. 2A and B. The main initial impurities were sulfur and carbon and these were easily removed by ion bombardment (2000 eV, 20 μA) resulting in a clean Rh surface spectrum of Fig. 2B. To maintain reproducible catalytic and adsorption activity, annealing was necessary, and a short anneal ($\sim$5 min @ 1000°C) was usually done, although this was minimized because of the segregation of an impurity ($\sim$ 180 eV, boron) upon cooling the sample. This was presumed to be boron and not tantalum as it appeared also on rhodium-supported samples, and no higher energy Ta peaks were observable in the spectrum. Attempts were made to rid the sample of boron by repeated ion bombardments and temperature cycling, but a final solution was to ion-clean the sample, and minimize the annealing time to prevent segregation. No segregation was observed in the low temperature catalysis and adsorption experiments. The peak overlap between the Rh(260) peak and the C(270) peak was not reduced by lowering the modulation amplitude below 5 V rms, and was therefore a consequence of the natural peak widths and instrumental broadening. Quantitative analysis of carbon on these surfaces was therefore very difficult and was not attempted.

Removal of carbon by other methods such as high temperature oxygen treatment was tried, and found to be less effective than ion bombardment. A surprising observation after oxygen treatments was the lack of substantial oxygen Auger signals. The rhodium surfaces did not accumulate oxygen near the surface as easily as they accumulated carbon. In Fig. 2C is shown the Auger spectrum of the clean Rh surface, heated in O_2 (1×10^{-7} Torr) at 500°C for 10 min. Only a small oxygen emission is seen. It is shown below that surface oxygen on Rh is easily removed by H_2 or

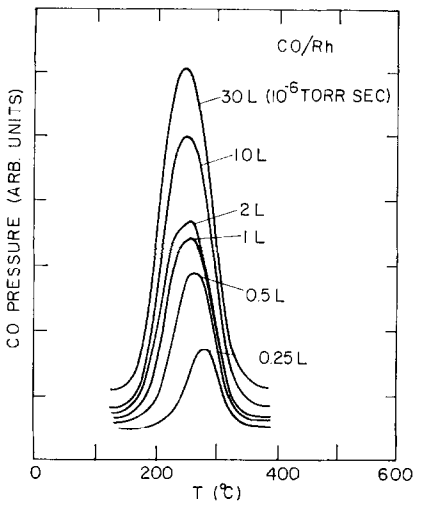

FIG. 3. Thermal desorption spectra of CO on Rh foils. Heating rate 25°C sec^{-1}, adsorption pressures 10^{-9}–10^{-5} Torr CO, at 300 K.

CO, and oxygen dissolved in the bulk is not detectable with Auger spectroscopy.

2. *Adsorption and Thermal Desorption of CO, CO_2 and CO–H_2 Mixtures*

CO was found to adsorb strongly on the polycrystalline Rh surfaces at low pressures (10^{-9}–10^{-4} Torr) and 300 K, but the adsorption behavior was markedly dependent on the surface pretreatment. Molecular, or α-CO desorbed around 250°C from the clean surface, and the thermal desorption spectra, as a function of coverage are shown in Fig. 3. These spectra were taken with a surface heating rate of 25°C/sec, and by preselecting the mass 28 peak in the quadrupole mass spectrometer. The surface saturated with CO between 10–30 L (I L = 10^{-6} Torr sec), and all of the CO desorbed as a single peak on the clean surface. This behavior is similar to observations of CO adsorption on other group VIII metals such as Ir (*6*) where CO also desorbs around 250°C.

It was found, however, that a single thermal desorption peak of the type in Fig. 3 was only obtained after scrupulously cleaning the Rh surface by ion bombardment. In particular, maintaining the surface at 800°C during Ar^+ ion bombardment was found to be necessary. If this was not done, a second CO thermal desorption peak was also present, around 700°C, as shown in Figs. 4 and 5. As discussed below this high temperature CO desorption peak is believed to be a recombination of adsorbed C and O atoms from dissociated CO, and the dissociation could be induced by adsorbing CO on a surface which was previously contaminated with C or O impurities (from previous experiments), or by preheating the surface in CO.

The desorption temperature of ~ 250°C indicates an activation energy for desorption of 32 ± 3 kcal, which is probably a reasonable estimate for the heat of adsorption on Rh. CO desorbs from iridium single crystals around 250°C (*6*) and a heat of adsorption measurement, based on a LEED structure, gave 35 kcal as the value on this

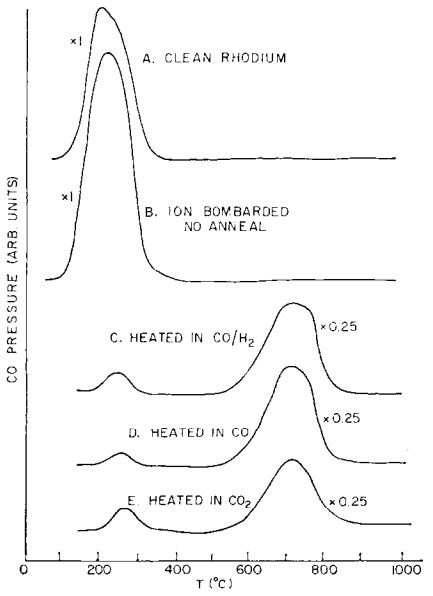

FIG. 4. Thermal desorption of CO from Rh after various treatments. (A) Clean surface, 30 L; (B) ion bombarded surface, 30 L; (C) heated in CO/H_2 1:1, 10^{-6} Torr, 300°C for 10 min; (D) as in (C), but pure CO; (E) as in (C) but pure CO_2.

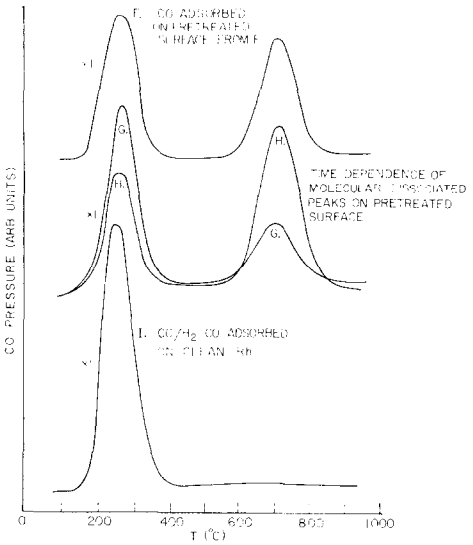

FIG. 5. Thermal desorption of CO from Rh after various treatments. (F) CO adsorbed on surface from Fig. 4E, 30 L; (G) CO adsorbed on (F) rapidly by 2×10^{-6} Torr CO, 15 sec; (H) CO adsorbed slowly from ambient on (H), for 120 min; (I) H_2/CO co-adsorbed (1:1, 1×10^{-6} Torr, 30 sec, 300 K) on clean surface.

metal (*7*). The 250°C peak on Rh is therefore certainly molecular, but the 700°C desorption peak is most probably a recombination of atomic carbon and oxygen. This hypothesis is supported by further experiments on Rh single crystals in this laboratory (*8*) and similar observations on a nickel (110) surface (*9*).

Figure 4A shows the desorption of CO around 250°C from the clean surface, prepared by the high temperature ion bombardment, and annealing. Figure 4B shows the effect of ion bombarding the surface, without annealing it: the amount of adsorbed CO is increased, but no new peaks appear, implying that this increase in CO adsorption is caused by a surface area increase. In Fig. 4C to E, the clean surface was heated in 10^{-6} Torr of CO/H_2 (1:1), CO and CO_2, respectively, for 10 min at 300°C. The scale on these spectra has been reduced by a factor of 4. A new CO thermal desorption peak, around 700°C, has appeared, and there is no significant difference in the spectra of 4C to E, indicating similar species on the surface. Both gas phase CO and CO_2 therefore dissociate on the clean Rh surface upon heating and hydrogen does not seem to be necessary for this process to occur.

After the thermal desorption spectrum of 4E was taken, CO was then readsorbed on this surface at 300 K and Fig. 5F resulted. Instead of a single peak, both molecular (250°C) and dissociated (700°C) CO desorbed. The presence of the dissociated CO however was related to the rate at which CO was adsorbed on the surface, and this is illustrated in Fig. 5G and H. Spectrum 5G was obtained by saturating the surface from 5F with CO at 2×10^{-6} Torr, and spectrum 5H was obtained by slowly adsorbing CO from the residual vacuum (1×10^{-9} Torr) over a period of 2 hr. In the case of the short exposure, the low temperature peak dominates, but for the slow adsorption, the high temperature peak dominates. The high temperature peak could again, be eliminated by Ar^+ ion bombardment at 800°C, followed by annealing. In spectrum 5I, a H_2–CO mixture (1:1) was adsorbed on the clean surface to

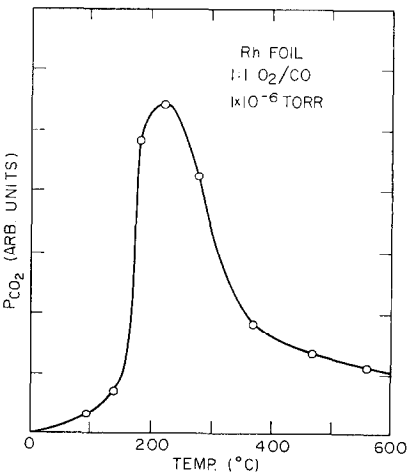

FIG. 6. Variation in the rate of CO_2 production with temperature, in the CO–O_2 reaction on Rh (10^{-6} Torr, 1:1).

saturation at 1×10^{-6} Torr and 300 K. The amount of low temperature CO on the surface significantly increased, but there were no apparent changes in binding energy of this state. Thus the presence of gas phase hydrogen does not appear to change the binding energy of adsorbed CO on the metal surface.

The Auger spectra of the Rh surface prior to adsorption of CO, when the high temperature peak was present, were identical to the clean surface. Therefore it is proposed that very low concentrations of C and O dissolved in the near-surface layers of rhodium may affect the CO desorption, by promoting the dissociation of molecular CO. The predominance of dissociated CO upon heating the sample in H_2–CO, CO, and CO_2, and the similarity of the thermal desorption spectra suggests that it is a layer of carbon and oxygen atoms, recombining and desorbing as carbon monoxide. No other species were detectable during these desorption experiments (e.g., CO_2).

Hydrogen adsorption was studied, and H_2 was found to desorb near room temperature, so accurate data were not taken. The outgassing of H_2 dissolved in the Ta holder was also a problem. From the previous spectra, hydrogen does not seem to play an important role in the CO dissociation process, although it did increase the amount of α–CO on the surface, during co-adsorption.

Carbon dioxide was found to adsorb on the clean surface of Rh, although when desorbed, or heated in a pressure of 1×10^{-6} Torr of CO_2, dissociation occurred and a high temperature CO desorption peak was seen, similar to that from heating in CO.

3. Low Pressure Catalysis Studies

In these experiments, the mass spectrometer was the detector, and a dynamic pressure of the reacting gases was established in the UHV chamber by adjusting the leak rate and the pumping speed. The amplitude of the detected masses is proportional to their rate of production in the chamber under these flow conditions.

In the first experiments, mixtures of H_2 and CO gas varying from 1:1 to 3:1 ratio were established in the chamber at pressures between 1×10^{-4} and 1×10^{-7} Torr. The sample temperature was raised as high as 600°C, but usually around 300°C, and a search was conducted through the entire mass range (1–60) to find new masses or changes in those present. At no time was there any evidence for hydrocarbon product formation under these conditions. In particular, no methane was detectable. However, this is not surprising, as the calculation in the Appendix shows that equilibrium partial pressures of CH_4 at those pressures are below the detection limit of the mass spectrometer ($<10^{-13}$ Torr).

Other mixtures of gases were tried, including H_2–O_2 and CO–O_2. H_2O formation was observed over a short period of time (several minutes) from the H_2–O_2 mixture (10^{-7} Torr, 1:1, 300°C), but no reliable kinetic data could be taken due to changes in the rate with time. The CO–O_2 reaction, however, was more reproducible and the reaction rate was measured as a function of temperature in Fig. 6. The only product was CO_2, and the amplitude of the mass 44 peak was measured as a function of temperature from room temperature to 600°C. The reaction rates were quite reproducible, showing no hysteresis as the temperature was cycled, and the surface appeared capable of sustaining the reaction indefinitely. The maximum in the rate vs temperature curve in Fig. 6 is similar to the curves observed on other transition metals, e.g., Ir (*6*).

The mechanism is believed to involve a surface reaction between oxygen and CO. Auger analysis during reaction showed that oxygen was present on the surface, but disappeared upon evacuation of the reactant gases. The importance of this mechanism to the understanding of the CO–H_2 reaction at high pressures, and an explanation

of the absence of $CO-H_2$ products at low pressures, are included in the Discussion.

B. Atmospheric Pressure Studies

1. *The Product Distribution and Surface Composition on the Clean Rhodium Surface*

The $CO-H_2$ reaction was investigated at 700 Torr total pressure, with the high pressure cell operating as a circulating batch reactor. Prior to isolation of the sample, it was Ar^+ ion bombarded at 800°C for 20 min, then annealed at 1000°C for 5 min in UHV ($<1 \times 10^{-8}$ Torr). The surface was then analyzed with AES. The high temperature ion bombardment was necessary to remove near-surface impurities (C, O, and S) introduced from previous experiments. Reproducible catalytic behavior was only possible with the above treatment.

In Fig. 7 we show the results of a 5 hr run at 300°C, 3:1 H_2/CO ratio and 700 Torr total pressure. The data are plotted as a hydrocarbon concentration in molecules per unit geometrical surface area of catalyst versus time. The slope of the line represents the rate of reaction. Turnover numbers, or molecules per surface site per second, may be calculated from this data if the number of active sites per square

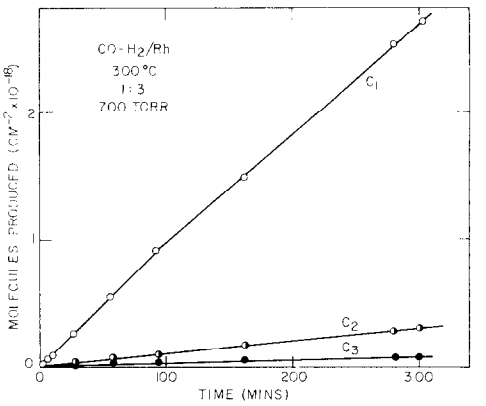

Fig. 7. Production of hydrocarbons from a 3:1 H_2/CO mix on rhodium foil (700 Torr, 300°C), with the internal isolation cell operated as a stirred batch reactor.

TABLE 1

Comparison of Polycrystalline Rh Foil with a 1% Rh/Al_2O_3 Catalyst in the $CO-H_2$ Reaction at Atmospheric Pressure

	Polycrystalline Rh foil (this work)	Supported 1% Rh/Al_2O_3 (Vannice) (*10*)
Reaction conditions	300°C, 3:1 H_2/CO 700 Torr	300°C[a], 3:1 H_2/CO 760 Torr
Type of reactor	Batch	Flow
Conversion (%)	<0.1	<5
Product distribution (%)	90 CH_4 ± 3 5 C_2H_4 ± 1 2 C_2H_6 ± 1 3 C_3H_8 ± 1 <1 C_4 +	90 CH_4 8 C_2H_6 2 C_3 <1 C_4 +
Absolute methanation rate at 300°C (turnover No.) (molecules $site^{-1}$ sec^{-1})	0.13 ± 0.03	0.034
Activation energy (kcal)	24.0 ± 2	24.0

[a] Data adjusted from 275°C.

centimeter is known; in the following text, 10^{15} sites/cm^2 was chosen as a rough value for comparison with other data, since the surface atom density of the polycrystalline rhodium sample cannot be measured accurately.

Under these reaction conditions, CH_4 was the dominant product, with smaller amounts of C_2 and C_3 products also detectable. Very small amount of C_4 products ($<1\%$) were also observed. The product distribution remained constant over the 5 hr period, and the rates of production essentially constant, which implies that poisoning effects due to product inhibition were not operative. There was no detectable induction period for this reaction, and the rates of formation were reproducible to within 5%, from run to run, provided the sample was cleaned in UHV prior to the experiment.

In Table 1 we compare these data from polycrystalline Rh at 300°C, and the data reported by Vannice (*10*) on a supported 1% Rh/Al_2O_3, catalyst adjusted to 300°C. Vannice's product distribution on supported Rh was measured at 265°C, but only a small difference is expected between this and 300°C. The product distributions are very similar, except that ethylene was observed as a product in this work, but not on the supported Rh. The absolute rates of reaction at 300°C agree within a factor of 4, and this is very reasonable considering the different methods of surface area measurement (hydrogen chemisorption versus geometrical measurement). This good agreement in catalytic behavior suggests that small surface area foils can be readily used as model catalysts for the CO–H_2 reaction.

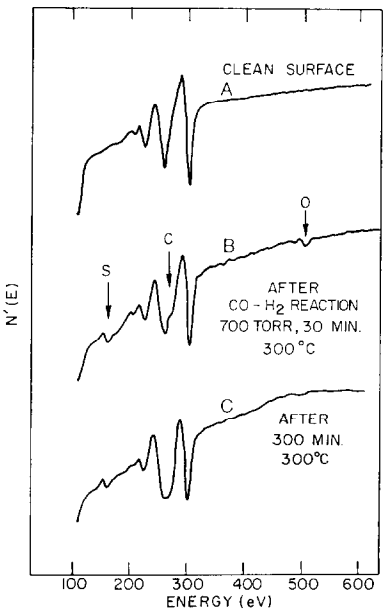

FIG. 8A. Auger analysis of the clean Rh surface; (B) the surface after 30 min reaction (300°C, 700 Torr, 3:1 H_2:CO); (C) the surface after 5 hr reaction.

After this experiment was performed at 1 atm, the sample was reexposed to UHV, and analyzed with AES to determine the surface composition. The results of these analyses are presented in Fig. 8. After reaction, the rhodium surface had some carbon present, and no oxygen, or only traces, were seen. Occasionally, small amounts of sulfur were observed on the surface. Figure 8 shows analyses after 30 min and after 5 hr of reaction at 300°C. The amount of carbon usually increased with time, and after 5 hr of reaction, the estimated surface concentration was probably ~1–2 monolayers, based on the attenuation of the rhodium peaks. The Auger analysis is not sensitive to subsurface impurities, however, and it is shown below that both carbon and oxygen are also incorporated into the bulk metal during reaction.

This carbon appeared to be in a form other than adsorbed CO, since it was removed only by heating the sample to 1000°C. The mechanism of removal was either by desorption, or diffusion into the bulk metal. The carbonaceous deposit did not appear to inhibit hydrocarbon production as Fig. 7 showed a constant production over a period when the surface changed from clean to one with the carbon layer present. The absence of surface oxygen is

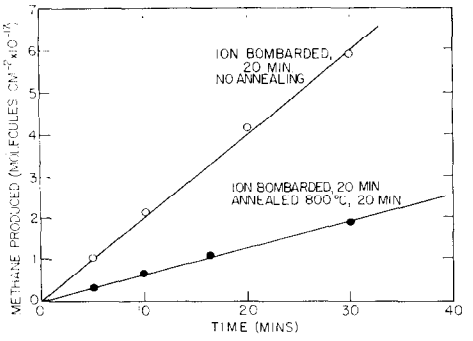

FIG. 9. Variation in methanation activity of Rh foil with ion bombardment pretreatment.

apparent, and the small Auger peak in Fig. 8 was the maximum ever observed after reaction. In the majority of runs, no surface oxygen was detectable. One possible reason for its absence, is the reaction of CO or H_2 with chemisorbed oxygen as the sample cooled down from reaction temperatures (250–350°C) to the region where the CO–O_2 and H_2–O_2 reactions were observed to have significant rates at low pressures (~200°C).

2. *The Variation in Methanation Rate with Ion Bombardment Pretreatment*

To obtain reproducible reaction rates on the foil samples, it was stated previously that a high temperature ion bombardment was needed, to rid the near-surface layers of C and O impurities from previous runs. It was found, however, that if the surface was not annealed reproducibly, or if high temperature was not used during bombardment, that large variations in reaction rates (up to a factor of 6) were possible. The first effect (annealing) is discussed in this section, and the effect of near-surface impurities is discussed below.

Figure 9 summarises the results. Only methane production is shown as the product distribution was the same as that from the annealed surface in all cases. The lower curve shows the rate of methane production at 300°C on a bombarded and annealed surface. The upper curve shows the rate on a bombarded surface only—the rate is a factor of 3 higher. This behavior agrees with the results of thermal desorption at low pressures and reflects the effects of surface roughness. A 5 min anneal at 1000°C was found to be sufficient for reproducible behavior; shorter anneals resulted in rates lying in between those indicated by the two curves. A standard surface treatment which removes surface damage was therefore essential in preparing ion bombarded samples for reaction.

3. *The Variation in Product Distribution and Reaction Rates with Temperature and CO–H_2 Ratio, on the Initially Clean Rh Surface.*

The variation of reaction rates and production distributions with CO–H_2 ratios and temperature were studied. For the methanation reaction, the data taken between 250 and 450°C with a 3:1 H_2:CO ratio are shown in Fig. 10. These data were extracted from experiments by increasing

TABLE 2

VARIATION OF REACTION PRODUCT DISTRIBUTION (%) with H_2/CO Ratio and Temperature, over Rh Foils[a]

Temp (°C)	Product	H_2/CO ratio		
		1:2	3:1	9:1
250 =	C_1	65	84	93
	$C_2(=)$	16	9	4
	C_2	9.8	3	2
	C_3 +	9.2	4	1
300 =	C_1	77	89	95
	$C_2(=)$	13	7	2
	C_2	4	2	2
	C_3 +	6	3	1
350 =	C_1	83	94	98
	$C_2(=)$	12	3	0
	C_2	1	2	2
	C_3 +	4	1	0.2

[a] C_1, methane; $C_2(=)$, ethylene; C_2, ethane; C_3, propane.

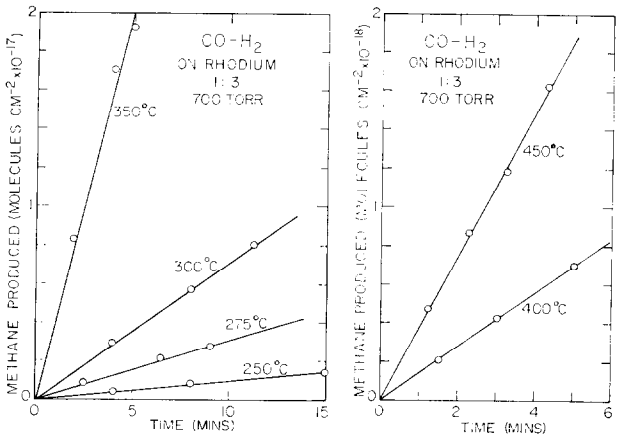

FIG. 10. Production of methane on initially clean rhodium foils as a function of temperature.

the sample temperature sequentially, and taking all the data in a single run. All of the rate curves are linear, and data were taken for a short time only to avoid possible poisoning effects at high temperatures. The Arrhenius plot, shown in Fig. 11 indicates an activation energy of 24 ± 3 kcal which is in excellent agreement with Vannice's value for the 1% Rh/Al_2O_3 catalyst under the same conditions.

To investigate whether the higher molecular weight hydrocarbons (C_2, C_3) were produced with the same activation energy, the H_2–CO ratio was varied between 0.5 and 9 and the reaction rates and product distributions of the various species followed between 250 and 350°C. Product distributions as a function of temperature and H_2/CO ratios are shown in Table 2. The general trend is that CH_4 is the dominant product under all conditions, that were employed, but the fraction of C_2 and higher molecular weight products increases with decreasing H_2/CO ratio and decreasing temperature. The most favorable conditions for chain growth from Table 2 are a 1:2 H_2/CO mixture at 250°C, and the most favorable methanation conditions are a 9:1 H_2/CO mixture at 350°C.

The product distribution has been truncated at C_3 (propane) because in most cases C_4's were <1% of the total products, and near the detection limit. Under favorable chain growth conditions, small amounts of C_4's and C_5's were seen, but are not listed in Table 2. These results are very similar to those reported by Vannice (*10*) on supported Rh, with one exception, and that is the type of C_2 product. In our experiments, ethylene [$C_2(=)$] was found to be the major product, with ethylene/ethane ratios as high as 12:1 under conditions of excess CO. Generally, the C_2H_4/C_2H_6 ratio

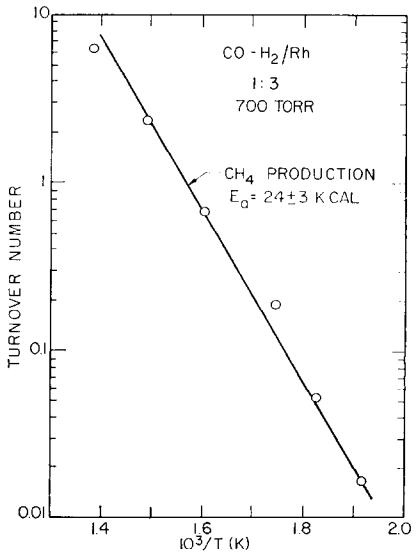

FIG. 11. Arrhenius plot for methane production on rhodium foils, from 250–450°C.

decreased at high H_2/CO ratios, but had different behavior as a function of temperature, depending on the H_2/CO ratio. At $H_2/CO = 0.5$, the C_2H_4/C_2H_6 ratio increased considerably with increasing temperature, but at $H_2/CO = 9$ it decreased dramatically at temperatures in excess of 300°C. In fact the ethylene appeared to be hydrogenating, as the concentration decreased with time at 350°C. The presence

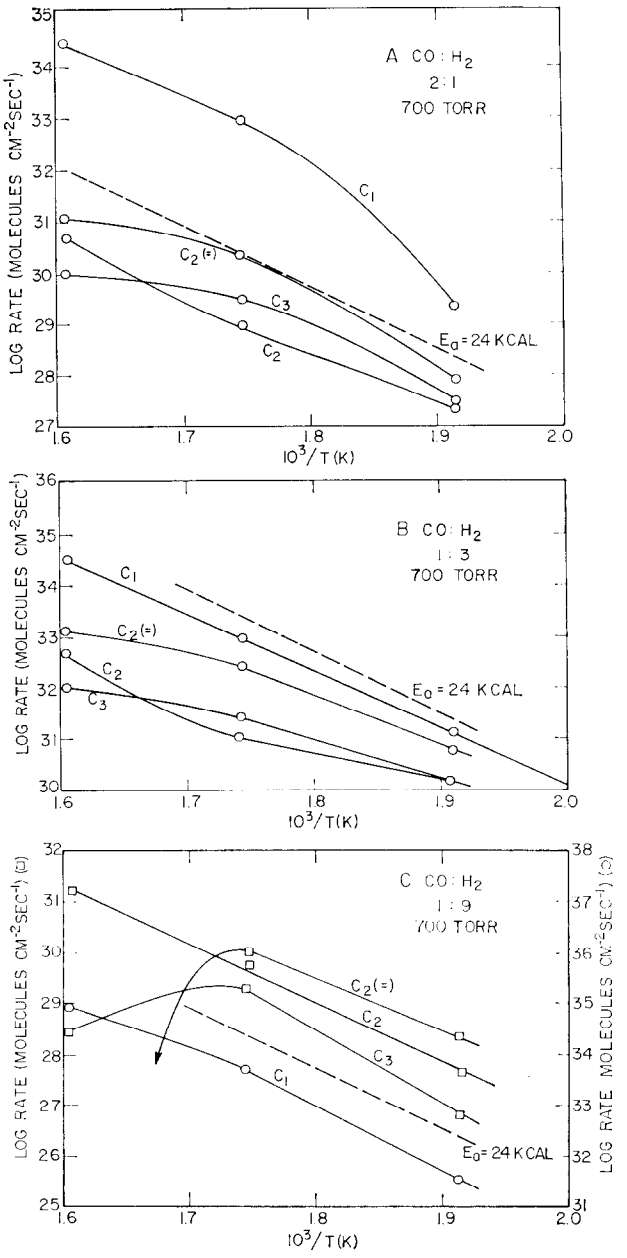

FIG. 12. Arrhenius plots for formation of hydrocarbons from $CO–H_2$ mixtures over rhodium foils at atmospheric pressure, and 250–350°C. (A) $CO:H_2 = 2:1$; (B) $CO:H_2 = 1:3$; (C) $CO:H_2 = 1:9$.

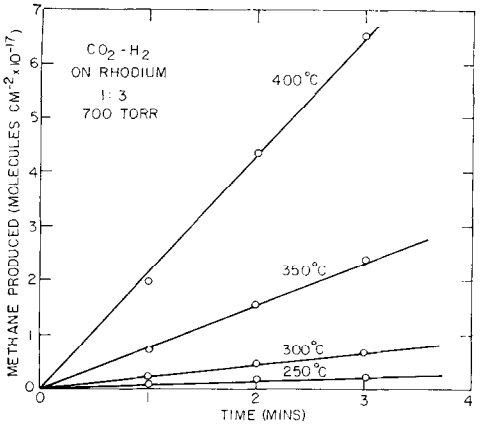

FIG. 13. Formation of CH_4 from CO_2–H_2 over Rh foil (1:3 ratio, 250–400°C, 700 Torr).

of ethylene as a major C_2 product contrasts with Vannice's data on supported Rh, in which he reported ethane as the dominant product, except at low hydrogen concentrations. This difference in product distribution may reflect the role of the alumina support, and is discussed below.

It was reported earlier that the activation energy for methanation was 24 ± 3 kcal, at a 3:1 H_2/CO ratio, and 250–450°C. The variation in reaction rates as a function of temperature, for the C_1–C_3 products, at the three H_2/CO ratios reported in Table 2, were also studied. The results are summarized in Fig. 12A, B, C where we show Arrhenius plots for all products at three H_2/CO ratios. The broken line corresponds to an activation energy of 24 kcal/mole of product, and is used as a reference. In general, detailed comparisons of "activation energies" will not be made, but several general features will be discussed. At 3:1 H_2/CO ratio (Fig. 12B), CH_4 forms with an activation energy of 24 ± 2 kcal, and this is also the value observed at H_2/CO = 9:1 (Fig. 12C). For a 1:2 ratio (Fig. 12A), the activation energy for methane formation apparently increases at low temperatures (<300°C), to about 24 kcal at higher temperatures. The methanation rates at 250°C are therefore lower than expected. These are also the conditions under which more chain growth is observed, however. Curvature of the Arrhenius plot is also observed for the C_2 and C_3 products. In general, the ethane activation energy apparently increases with temperature, except at 9:1 ratio, and ethylene has an apparent decrease in activation energy with temperature; in fact in Fig. 12C at temperatures in excess of 300°C, gaseous ethylene hydrogenates to ethane, and a negative rate of C_2H_4 production results. For propane, an increase in temperature also produces a curved Arrhenius plot, with a decrease in activation energy, particularly above 300°C.

To summarize these results, a fairly similar temperature dependence of the reaction rate is observed for all products below 300°C, but above this temperature, hydrogenation of ethylene to ethane, and smaller rates of C_3 production are observed. Methane formation, however, proceeds with a constant activation energy

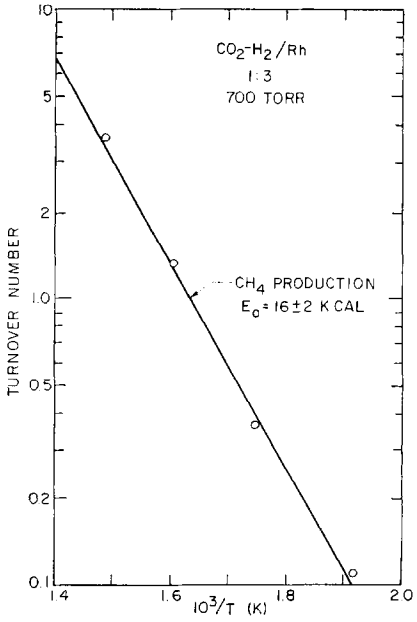

FIG. 14. Arrhenius plot for methane production from CO_2–H_2 on Rh (1:3 ratio, 250–400°C, 700 Torr).

even to 450°C, as measured previously in Fig. 11.

The variation of reaction rates with partial pressures of CO and H_2 was not studied. Vannice's data on 1% Rh/Al_2O_3 (*10*) showed that the methanation rate was proportional to the first power in hydrogen, and a small negative exponent for CO, and these results were similar for most of the other group VIII metals.

4. Reaction Rates and Product Distributions for the CO_2–H_2 Reaction on the Initially Clean Rh Surface

As a parallel study, CO_2–H_2 mixtures were reacted on clean Rh surfaces, prepared in the same way as for the CO–H_2 studies. All reactions were carried out at 700 Torr, and temperatures between 250 and 400°C, with CO_2–H_2 ratios between 1:1 and 1:10. Two specific observations were made, first, that the CO_2–H_2 reaction is *highly selective* for CH_4 formation, with little or no C_2 or higher molecular weight products ever observed. Second, the specific reaction rates for the CO_2 reaction were always higher than for CO under the same conditions.

For a 3:1 H_2/CO_2 mixture, at 700 Torr, the reaction rates (CH_4 formation) and Arrhenius plot are shown in Figs. 13 and 14, respectively. The activation energy for CH_4 formation from CO_2 is 16 ± 2 kcal, which is considerably lower than that measured for methanation from CO–H_2 under the same conditions. As a direct comparison of the activities of the CO–H_2 and CO_2–H_2 reactions on the initially clean Rh surface, Table 3 compares the activation energies, for CH_4 formation, and specific methanation rates at 250 and 300°C. The CO_2–H_2 reaction is more active than the CO–H_2 reaction at lower temperatures, with the rate approximately seven times that for the CO–H_2, at 250°C. It can be seen that the CO_2–H_2 reaction is certainly more active in the lower temperature range. The methanation rates for the two reactions only become comparable around 440°C, due to the large difference in activation energies.

TABLE 3

Comparison of Activities for Methanation of the CO–H_2 and CO_2–H_2 Reactions on the initially Clean Rh Surface (1:3 Ratio, 700 Torr).

	CO–H_2 = 1:3	CO_2–H_2 = 1:3
Specific rate at 250°C (turnover No.) (CH_4 molecules $site^{-1}$ sec^{-1})	0.017	0.12
Specific rate at 300°C	0.13	0.36
Activation energy (kcal)	24 ± 2	16 ± 2

Auger analyses of the Rh surfaces, after treatment with CO_2–H_2 mixtures, were carried out, and the results were identical to the spectra in Fig. 8. A carbonaceous deposit developed during the reaction, while no oxygen was seen near the surface. This carbonaceous deposit did not inhibit the reaction, and CO_2–H_2 mixtures could be catalyzed for several hours without a noticeable decline in the methanation activity. Variations in the H_2/CO ratio did not produce any detectable changes in the surface analysis after reaction, and methane was almost always the exclusive product formed.

5. Comparison of the CO–H_2 and CO_2–H_2 Product Distributions and Rates on Pretreated Rhodium Surfaces

In the initial stages of this work it was discovered that the specific reaction rates on the Rh surface were dependent on the pretreatment of the surface with various gases. In certain cases, Auger spectroscopy revealed no obvious surface impurities as being responsible for these variations, however, the effects were quite reproducible,

and apparently caused by subsurface impurities. To quantify these effects, a series of eight experiments was conducted, to measure the specific reaction rates and product distributions, on these pretreated surfaces, and to compare these results with those obtained on the clean surface.

Each pretreatment consisted of heating the clean Rh surface for 15 min at 300°C in 1 atm of a particular gas (O_2 CO or C_2H_2), then exposing the surface to vacuum and flashing to 1000°C to remove any adsorbed gases. The pretreated surface was then used to catalyze the CO–H_2 and CO_2–H_2 reaction (1:3, 300°C, 700 Torr) for 30 min. Auger spectroscopic analyses were carried out before and after reaction to monitor changes in surface composition, and the reaction layer was thermally desorbed in UHV after the high pressure runs. Each pretreatment, however, was preceded by a high temperature ion bombardment and annealed to remove surface impurities from the previous run and enable unambiguous interpretation of the data.

TABLE 4

Variation in Methanation Activity, and Product Distributions for the CO–H_2 and CO_2–H_2 Reactions on Clean and Pretreated Rhodium Surfaces[a]

Reaction gases	Surface[b] pretreatment	Methanation rate (300°C) (turnover No.)	Product distribution (%)
CO–H_2	None	0.15 ± 0.05	88 C_1 9 C_2 3 C_3
CO_2–H_2	None	0.33 ± 0.05	100 C_1
CO–H_2	O_2	0.33 ± 0.05	87 C_1 10 C_2 3 C_3
CO_2–H_2	O_2	1.7 ± 0.2	98 C_1 2 C_2
CO–H_2	CO	0.15 ± 0.05	88 C_1 9 C_2 3 C_3
CO_2–H_2	CO	0.33 ± 0.05	100 C_1
CO–H_2	C_2H_2	0.07 ± 0.02	78 C_1 18 C_2 4 C_3
CO_2–H_2	C_2H_2	0.07 ± 0.04	96 C_1 3 C_2 1 C_3

[a] Reaction conditions: 1:3 ratio, 700 Torr, 300°C.

[b] Heated for 15 min in 700 Torr of the particular gas, then thermally desorbed to 1000°C *in vacuo* before reaction.

The data for the methanation rates and the product distributions on the various surfaces are tabulated in Table 4. As a first observation, a variation in methanation activity of a factor of 10 was observed, the most active synthesis occurring for the CO_2–H_2 reaction on an oxygen-treated surface and the least active being the CO–H_2 reaction on an acetylene-treated surface. In general, the CO_2–H_2 reaction was *always* more active than the CO–H_2 reaction on the same surface, and oxygen pretreatment increased methanation rates, while carbon (from C_2H_2) retarded methanation, relative to the clean surface. The surface pretreated with CO was identical in methanation activity to the clean surface, for both reactions. Taking a closer look at Table 4, the methanation activity for the CO–H_2 reaction on the O_2-treated surface was the same as CO_2–H_2 on the clean surface. The kinetics for the CO_2–H_2 on the C_2H_2-treated surface were nonlinear with time, and the rate after 30 min was similar to CO–H_2 on this surface.

Auger analyses of the surface composition, after pretreatment and prior to reaction did not reveal significant differences to account for this large variation in catalytic behavior. Surfaces treated with oxygen and CO showed no carbon or oxygen peaks after the pretreatment and after

flashing *in vacuo* to 1000°C. Surfaces treated in acetylene, however, showed significant carbon peaks before and after flashing, and it is likely that this carbon was in the form of a graphitic overlayer. After the high pressure synthesis studies were carried out for 30 min, all surfaces had similar Auger spectra with carbon being the main surface impurity besides Rh. No oxygen was detectable on the surface.

The product distributions from the pretreated surfaces also showed differences. Surfaces treated with oxygen or CO showed essentially the same product distributions as the clean Rh foils, and in all cases, the CO_2–H_2 reaction was highly selective towards CH_4 formation. On the acetylene-treated surface, a higher percentage of C_2 and C_3 products resulted from the reduced methanation activity. Surface carbon formed by decomposing acetylene, therefore reduces methanation but does not affect chain growth significantly.

Each of the eight pretreated rhodium surfaces in Table 4 were studied by thermal desorption into UHV after the high pressure catalysis runs. The mass 28 emission was monitored as a function of temperature, and the resulting desorption spectra are shown in Fig. 15. In all cases, only mass 28(CO) was observed during desorption although H_2 desorption was occurring, but was not measured for reasons cited previously. For the reaction of CO–H_2 on the clean surface, both the low temperature peak, and the high temperature desorption was observed (Fig. 15A), indicating both molecular and dissociated CO present. For the CO_2–H_2 reaction, a very similar spectrum was seen, with the low temperature and high temperature CO desorbing (Fig. 15B). These may be compared with Fig. 15C, which was obtained after heating the clean surface in pure CO at 1 atm and 300°C for 30 min. This spectrum is very similar to the previous two and indicates that the dominant surface species seen after reaction are similar for the CO–H_2 and CO_2–H_2 reactions, and consist of molecular CO and dissociatively adsorbed CO. The total amount of CO desorbed after these runs was approximately 5–10 times that obtained by adsorbing CO on the clean surface at low pressures, and suggests that many of the C and O atoms are also incorporated into the near-surface layers.

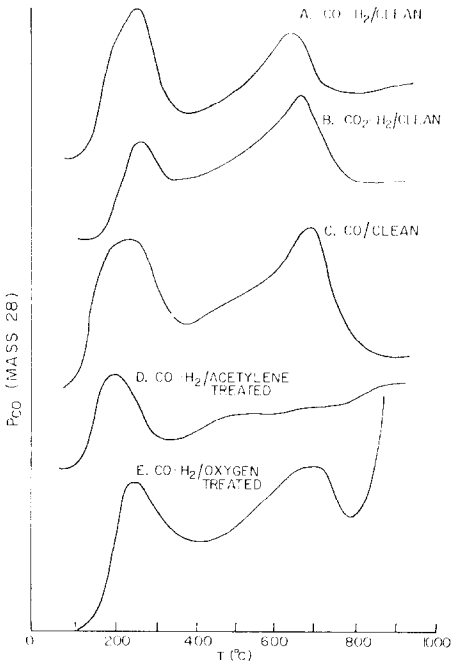

FIG. 15. Thermal desorption of pretreated Rh surfaces after CO–H_2 and CO_2–H_2 reactions (1:3 ratio, 700 Torr, 300°C).

The thermal desorption spectra for the acetylene-treated and oxygen-treated surfaces are seen in Fig. 15D and E, respectively. For the C_2H_2 case, molecular CO but no significant high temperature peak is seen, although continuous desorption of CO occurred over the entire temperature range. The total amount of high temperature CO desorbed in this case is much less than from the CO–H_2 reaction on the other pretreated surfaces and this correlates with the lowest methanation activity. Chain growth rates were unaffected on this surface, however. Rhodium pretreated with oxygen gave both the low and high tem-

perature CO peaks as shown in Fig. 15E, but a large emission of CO was also observed above 800°C and this is almost certainly due to dissolved oxygen reacting with carbon, and liberating CO. The presence of this large CO desorption was the only evidence obtained which supports the contention that excess dissolved oxygen is responsible for the increased methanation activity.

To summarize this data, oxygen pretreated rhodium surfaces have an enhanced methanation activity for both the $CO–H_2$ and $CO_2–H_2$ reactions, relative to the clean surface. This oxygen is undetectable by Auger spectroscopy, and does not change the product distribution, but becomes apparent when it reacts with carbon at temperatures in excess of 800°C and desorbs as CO. Carbon, introduced onto the surface from acetylene, probably in the form of a graphitic overlayer, reduces methanation activity relative to the clean surface, but does not affect chain growth. Thermal desorption spectra show that a significantly smaller proportion of dissociated CO is present on this surface. The clean surface, and CO treated surfaces, show methanation activities which are in between these two extremes, and thermal desorption spectra show both molecular and dissociated CO present. The $CO_2–H_2$ reaction is consistently faster than the $CO–H_2$ reaction on any of these surfaces, but the thermal desorption spectra after reaction look identical.

6. Reaction of Hydrogen with Clean and Pretreated Rh Surfaces at 1 atm

In the course of several experiments, pure hydrogen was reacted with the Rh surface to observe any product formation from the surface carbon layer. The first experiments involved running the $CO–H_2$ reaction on the clean surface for 30 min under standard conditions (3:1 H_2:CO, 300°C, 700 Torr) then pumping out the gases at 20°C and exposing the cell to UHV to remove any adsorbed CO. Pure H_2 was then admitted to the central cell and it was flushed several times to purge any remaining CO. The sample was then heated to 300°C in 800 Torr of hydrogen. Methane formation was observed, and curves similar to that shown in Fig. 16 were seen. Methane was evolved, the total quantity being many "monolayers" ($\sim$60 in Fig. 16) and this implies a substantial amount of carbon removed from the sample, not only from the surface, but from the bulk as well. No other products were seen. If cleaned Rh samples (cleaned by Ar^+ ion bombardment) were hydrogenated, no methane was seen up to 450°C or so. It appears, therefore that surface or bulk carbon produced during the $CO–H_2$ reaction may be hydrogenated to form methane on polycrystalline rhodium foils as low as 300°C.

Similar experiments were carried out on Rh surfaces pretreated with acetylene where considerable amounts of carbon as determined by AES (in excess of that produced in the $CO–H_2$ reaction) were deposited. The hydrogenation at 300°C as shown in Fig. 17, produced only methane, but the rate of production was slower than from the $CO–H_2$ treated surface, although it did not cease hydrogenating over the 30 min period. Raising the temperature to 375°C produced a significant increase in methane production, and the activation energy for this process, calculated from Fig. 17 is 21 $\pm$ 3 kcal, which is similar to the value observed for methane production from the $CO–H_2$ mix.

Hydrogen, therefore, can produce methane from surface, or bulk carbon on rhodium in the temperature range (300°C) that the $CO–H_2$ reaction is active, although the type of carbon deposited may affect the hydrogenation activity. The low activity at 300°C of the acetylenic carbon suggests that this may be in the form of a graphitic overlayer, which is resistant to hydrogenation. The carbon resulting from

dissociated CO appears to be more active in the hydrogenation to methane.

IV. DISCUSSION AND SUMMARY

We shall summarize the experimental findings that are useful to unravel the mechanism of hydrocarbon production from CO–H_2 and CO_2–H_2 mixtures.

a. There are two types of CO on polycrystalline rhodium, with widely differing desorption temperatures (250 and 700°C). Both states are present after reaction with CO–H_2 and CO_2–H_2 mixtures, but hydrogen is not necessary to produce the high temperature state. The thermal desorption spectra after heating in CO alone look identical to the CO–H_2 and CO_2H_2 cases. Pretreatment of the surface with acetylene reduces the high temperature state.

b. The active rhodium surface is covered with a carbonaceous deposit under reaction conditions and both carbon and oxygen are dissolved in the bulk metal, as evidenced by CO desorption at high temperatures. Little or no oxygen is present on the surface after reaction. Interaction of hydrogen with the surface after CO–H_2 catalysis produces only methane.

c. Any oxygen present in the reaction layer during synthesis must be removed rapidly by CO or H_2 to form CO_2 or H_2O, as these reactions (particularly the CO–O_2 reaction) are rapid at low pressures and temperatures.

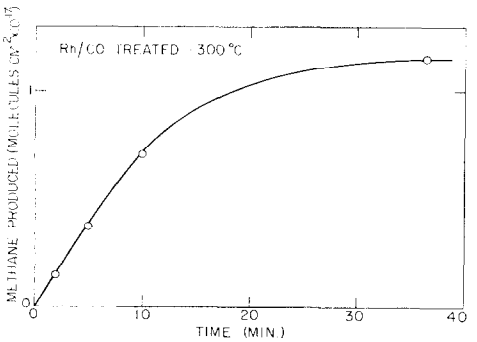

FIG. 16. Hydrogenation of the carbon residues produced in the CO–H_2 reaction on Rh (3:1 H_2:CO, 700 Torr, 300°C, 30 min, then hydrogenated with 800 Torr H_2, 300°C).

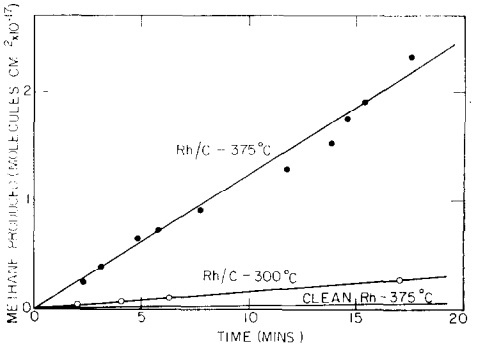

FIG. 17. Hydrogenation of surface carbon formed by decomposing acetylene on the Rh surface (pretreated with 800 Torr C_2H_2, 300°C, 15 min, then hydrogenated with 800 Torr H_2, 300°C).

d. The methanation rates, product distribution and activation energy for methanation from CO–H_2 mixtures agree well with that reported for a supported, dispersed rhodium catalyst. The major difference lies in the production of ethylene as the major C_2 product on Rh foils at less than 300°C.

e. The reaction of CO_2–H_2 mixtures on the initially clean Rh surface produces methane only, and at a faster rate, with a lower activation energy (16 kcal). At low temperatures ($\leq$ 250°C) the CO_2–H_2 methanation rate is an order of magnitude higher than the equivalent CO–H_2 rate.

f. The pretreatment of the rhodium surface with oxygen or acetylene markedly changes the rate and/or product distribution. Oxygen increases the rate of CH_4 formation by more than a factor of five from CO_2–H_2 mixtures, while acetylene reduces methanation, but not chain growth.

Hydrogen–carbon monoxide interactions have been investigated recently on metal single crystals and films. Wedler *et al.* (*11*) interacted H_2 and CO on nickel films at temperatures as high as 353 K. They observed no reaction products desorbed at

low pressures, but found a considerable increase in the amount of CO adsorbed in the presence of hydrogen at 353 K. Other work on (111) platinum (*12*) at low pressures showed slight changes in the thermal desorption spectra of a co-adsorbed CO–H_2 mixture, and EID evidence of a surface "complex" containing carbon, hydrogen and oxygen. On a (100) tungsten surface (*13*) Yates and Madey found evidence for significant interactions between adsorbed H_2 and CO, but could find no methane or any other hydrocarbon products desorbed. In this work, we observed an effect similar to that of Wedler *et al.*, namely an increase in the amount of CO adsorbed in the presence of hydrogen at low pressures, but desorption of methane, or any other hydrocarbon products were absent, even in catalysis experiments.

Thermodynamically, the formation of methane and higher molecular weight products from CO–H_2 mixtures at atmospheric pressure is quite favorable in the temperature range of interest (250–350°C) (*14*). At low pressures, however, the thermodynamics is quite unfavorable and this is outlined in the Appendix. This is simply a consequence of the pressure dependence of a condensation reaction, which is favored only by an increase in pressure. It is not surprising, therefore, that at low pressure, catalysis products are absent in the CO–H_2 reaction, and the importance and necessity of studying this reaction at atmospheric pressure and above is apparent.

Evidence is presented in this work to show that CO may dissociate under reaction conditions, and that the working catalyst surface is covered with molecular carbon monoxide and some strongly bound carbon, which is a result of the dissociation process. It is also apparent that there is a considerable amount of both carbon and oxygen dissolved in the rhodium bulk, near the surface. This is not readily detected with Auger spectroscopy, but appears as molecular carbon monoxide around 700°C when the surface is heated. Hydrogen does not not seem to be a necessary agent for dissociation of CO, or incorporation of carbon and oxygen into the bulk, as merely heating the sample in pure CO at 700 Torr generates similar desorption spectra.

Recent results from this laboratory (*8*) have simulated this recombination of carbon and oxygen on Rh single crystal surfaces by adsorbing oxygen on carbon-contaminated crystals. When these surfaces are heated the evolution of CO around 700°C occurs, in a similar fashion to the foils. The kinetics of this process, however, is not a simple second order one, as it depends upon the relative concentrations of carbon and oxygen in the bulk, and on the surface.

The presence of a carbonaceous deposit on the rhodium surface during the synthesis reactions, and the complete absence of oxygen in the Auger spectra is surprising, as rhodium oxides are thermodynamically stable, while the carbides are unstable (*15*). The carbonaceous layer must therefore consist of some Rh–C complex which forms in preference to a surface oxide. Some oxygen is incorporated into the rhodium surface during reaction, however, as evidenced by desorption of a high temperature form of CO after reaction, although it is not detectable with AES. Even after oxygen treatment at high pressures (1 atm) and heating to 300°C, only small oxygen Auger emissions were seen, indicating submonolayer coverage at the surface. This oxygen pretreatment does, however, have a marked influence on the rates of methanation on this surface indicating that excess subsurface oxygen can influence the reaction. The Auger spectra after reaction on these oxygen-treated surfaces showed the same carbonaceous overlayer observed in all experiments. We therefore conclude that excess ocygen, dissolved in the rhodium lattice below the surface promotes the methanation reaction without significantly influencing the product distribution.

Wanke and Dougharty (*16*) have observed uptakes of oxygen on supported rhodium catalysts in excess of one monolayer, at temperatures similar to Fischer–Tropsch conditions. This observation supports the contention that oxygen may penetrate the rhodium lattice, both during the catalysis with CO–H_2 mixtures, and during pretreatment with molecular oxygen at high pressures. A possibility for the effect of excess dissolved oxygen on the enhanced catalytic activity of rhodium is that faceting of the surfaces occurs, which may roughen the surfaces, increasing the surface area, or introduce new crystal planes of higher reactivity. Tucker (*17*) in fact has observed faceting of rhodium single crystals during the adsorption of oxygen.

The total absence of oxygen in the surface layer after reaction is easily explained with reference to the low pressure CO–O_2 and H_2–O_2 experiments. Both these reactions proceed at low temperatures and pressures (10^{-7} Torr and 100°C) and the removal of surface oxygen to form CO_2 and H_2O at atmospheric pressure is expected to be rapid. In fact experiments on supported rhodium catalysts near atmospheric pressure have shown that the CO–O_2 and H_2–O_2 reactions do proceed rapidly (*18*). The lifetime of an oxygen atom on the rhodium surface under Fischer–Tropsch conditions is therefore short, as the strongly bound carbon overlayer rapidly forms, preventing surface oxide formation, and oxygen atoms may either dissolve in the subsurface layers or be hydrogenated. This mechanism is supported by the observation of a complete absence of oxygenated hydrocarbons in the synthesis under our conditions of the experiment.

There is excellent agreement between the methanation rates and activation energies reported here, and by Vannice (*10*) for supported, dispersed rhodium catalysts (Table 1). This is gratifying as we can now use small surface area rhodium foils as model systems, representative of high surface area rhodium catalysts. The product distribution is somewhat different; more ethylene forms in the absence of the high surface area support. Future studies should verify whether the support is indeed responsible for the hydrogenation of unsaturated hydrocarbons, thereby partly masking the catalytic behavior of rhodium.

One of the significant findings of this study is the marked increase in selectivity to methane when CO_2 is used as a reactant instead of CO. The chain growth is arrested completely, although the AES analysis shows a similar carbonaceous deposit after reaction. The methanation rates, however, are more rapid than CO at temperatures <440°C, as the activation energy is 16 kcal as opposed to 24 kcal for the CO–H_2 reaction. The excess chemisorbed oxygen that forms as a result of partial dissociation of CO_2 therefore has a different effect than pretreating the surface with oxygen. It appears that with CO_2 as a reactant either the nature of the surface intermediates in the reaction is altered significantly, or atomic oxygen disperses the carbon species on the surface, increasing the selectivity to methane formation. Another explanation is that atomic oxygen blocks sites responsible for chain growth, or that the metal–carbon complex that forms is rehydrogenated rapidly enough to minimize the surface concentration of partially hydrogenated species that could link up to form higher molecular weight products. Clearly, unraveling the nature of the surface intermediates that form during the CO_2–H_2 reaction should help us control chain termination in the Fischer–Tropsch reaction.

The hydrogenation of CO_2 to methane has been investigated by other workers but the mechanism is not well understood. On a ruthenium catalyst, Lunde and Kester (*19*) found an activation energy of 16.84 kcal for CO_2 hydrogenation, which is in good agreement with our value of 16 kcal for a Rh foil. Karn *et al.* (*20*) found the

same high selectivity to methane for this reaction, even at 21.4 atm over a ruthenium catalyst. Under similar pressures, CO produced high molecular weight waxes. It is therefore encouraging that these foil surfaces can reproduce the product distributions and kinetics of supported catalysts. The mechanism of CO_2 hydrogenation, therefore seems to be linked to the role of the extra oxygen atom in the surface intermediates, as there are no apparent differences between the working catalyst surfaces in the CO–H_2 and CO_2–H_2 reactions, as determined by AES and thermal desorption.

The pretreatments of the surface have marked and controlling effects on both the reaction rates and product distributions. While oxygen pretreatment increases the CO_2–H_2 rate fivefold, acetylene pretreatment reduces methanation but not chain growth in both the CO_2 and CO–H_2 reactions. These observations indicate that the surface composition and perhaps also the surface structure that is predetermined by the oxygen or acetylene pretreatments control the rate and product distribution in the Fischer–Tropsch reaction. Since the surface is covered with a carbonaceous overlayer during the reaction it is reasonable to conclude that the structure and nature of the rhodium–carbon bonding determines the reaction rate and path. The carbon on the rhodium surface is active; we have shown that it rehydrogenates readily to form methane. It appears that these rhodium–carbon or rhodium–carbon–oxygen compounds at the surface are those that react with hydrogen to form the products.

The hydrogenation, or gasification of carbon using rhodium as a catalyst has been investigated by Tomita *et al.* (*21*). The conversion of carbon to CH_4 occurred at temperatures in excess of that in the Fischer–Tropsch reaction, but much lower than that required to directly hydrogenate carbon in the absence of a catalyst. Rhodium was the most efficient gasification catalyst investigated.

We cannot deduce the exact nature of the reaction intermediates in the CO–H_2 reaction without further experiments. It is significant, however, that both molecular and dissociated carbon monoxide are present under synthesis conditions. It is also significant that large amounts of carbon at the surface (from decomposed acetylene) retarded methanation, but did not affect chain growth. The high temperature, or dissociated CO, was much less evident on these surfaces, while molecular CO was present. There may in fact be a distinction between the methanation reaction, and the chain growth reaction, as methane can be produced readily, from carbon but chain growth products require the presence of adsorbed molecular CO. In fact recent work by Wentrcek *et al.* (*22*) indicates that that reactive carbon on nickel can be hydrogenated directly to methane.

Future studies will be carried out with single crystals to determine the effect of surface structure on the reactivity, and elevated pressures will be used to increase the chain growth probability and investigate this mechanism further. Since the surface composition of the catalyst appears to be all-important in the Fischer–Tropsch reaction on rhodium, other transition metals should also be scrutinized to explore the presence of similar effects. Photoelectron spectroscopy and high resolution energy loss spectroscopy appear promising techniques to identify the bonding of various metal–carbon surface complexes.

APPENDIX

The Pressure Dependence of the Equilibrium of a Condensation Reaction (*23*)

For the reaction

$$aA + bB \rightarrow cC\,d + D \qquad (1)$$

The equilibrium constant in terms of partial fugacities is

$$K_f = \frac{(f_C)^c(f_D)^d}{(f_A)^a(f_B)^b}. \quad (2)$$

In terms of partial pressures, this becomes

$$Kp = \frac{(Px_C)^c(Px_D)^d}{(Px_A)^a(Px_B)^b}, \quad (3)$$

where p = total pressure and x_A, x_B are mole fractions. It follows that

$$K_f = K_p \cdot K_\gamma, \quad \text{where} \quad \gamma = f/P, \quad (4)$$

and

$$K_\gamma = \frac{(\gamma_C)^c(\gamma_D)^d}{(\gamma_A)^a(\gamma_B)^b}. \quad (5)$$

We approximate $K_\gamma \approx 1$ for Fischer–Tropsch reaction conditions (<100 atm). Then

$$\frac{(x_C)^c(x_D)^d}{(x_A)^a(x_B)^b} \cong K_f \cdot P^{-\Delta n}, \quad (6)$$

where

$$-\Delta n = (a + b) - (c + d).$$

Thus condensation reactions, where $a + b > c + d$ are favored by a pressure increase. For all of the Fischer–Tropsch reactions, $a + b > c + d$ is the general rule.

As an example, for the reaction

$$3H_2 + CO \rightarrow CH_4 + H_2O.$$

$$(\Delta G_f)\ 430°C,\ 1\ \text{atm} = -11.42\ \text{kcal}$$

$$\therefore \quad K_f = 3.68 \times 10^3.$$

At 10^{-4} Torr total pressure,

$$K_f \cdot P^2 = 3.68 \times 10^3 \times 1.73 \times 10^{-14} = 6.4 \times 10^{-11}.$$

The equilibrium methane concentration under these conditions would therefore be very low ($\sim 10^{-13}$ Torr).

ACKNOWLEDGMENT

This work was done with support from the United States Energy Research and Development Administration.

REFERENCES

1. Pichler, H., "Encyclopedia of Chemical Technology" (R. E. Kirk and D. F. Othmer, Eds.), 2nd ed., Vol. 4, p. 450. Wiley (Interscience), New York, 1964.
2. Mills, G. A. and Steffgen, F. W., *Catal. Rev.* **8**, 159 (1973).
3. Natta, G., in "Catalysis" (P. H. Emmett, Ed.), Vol. 3, Reinhold, New York, 1955.
4. Anderson, R. B., *in* "Catalysis" (P. H. Emmett, Ed.), Vol. 4. Reinhold, New York, 1956.
5. Blakely, D. W., Kozak, E. I., Sexton, B. A., and Somorjai, G. A., *J. Vac. Sci. Technol.* **13**, 1091 (1976).
6. Hagen, D. I., Nieuwenhuys, B. E., Rovida, G., and Somorjai, G. A., *Surf. Sci.* **57**, 632 (1976).
7. Comrie, C. M., and Weinberg, W. H., *J. Chem. Phys.* **64**, 250 (1976).
8. Unpublished data, this laboratory.
9. Price, G. L., Sexton, B. A., and Baker, B. G., *Surf. Sci.* in press.
10. Vannice, M. A., *J. Catal.* **37**, 462 (1975).
11. Wedler, G., Papp, H., and Schroll, G., *J. Catal.* **38**, 153 (1975).
12. Baldwin, V. H., and Hudson, J. B., *J. Vac. Sci. Technol.* **8**, 49 (1971).
13. Yates, J. T., Jr., and Madey, T. E., *J. Chem. Phys.* **54**, 4969 (1971).
14. Storch, H. H., Golumbic, N., and Anderson, R. B., "The Fischer–Tropsch and Related Syntheses" Wiley, New York, 1951.
15. Searcy, A. W., *in* "Chemical and Mechanical Behavior of Inorganic Materials" (A. W. Searcy, D. V. Ragone and U. Colombo, Eds.), p. 1. Wiley (Interscience), New York, 1970.
16. Wanke, S. E., and Dougharty, N. A., *J. Catal.* **24**, 367 (1972).
17. Tucker, C. W., Jr., *Acta Met.* **15**, 1465 (1967).
18. Taylor, K. C., private communication.
19. Lunde, P. J., and Kester, F. L., *J. Catal.* **30**, 423 (1973).
20. Karn, F. S., Schultz, J. F., and Anderson, R. B., *Ind. Eng. Chem. Prod. Res. Develop.* **4**, 265 (1965).
21. Tomita, A., Sato, N., and Tamai, Y., *Carbon* **12**, 143 (1974).
22. Wentrcek, P. J., Wood, B. J., Wise, H., *J. Catal.* **43**, 363 (1976).
23. Newton, R. H., and Dodge, B. F., *Ind. Eng. Chem.* **27**, 577 (1935).